Vol. 562: 123–134, 2016
doi: 10.3354/meps11958

MARINE ECOLOGY PROGRESS SERIES
Mar Ecol Prog Ser

Published December 29

Widespread physical mixing of starry ray from differentiated populations and life histories in the North Atlantic

A. Lynghammar[1,*], K. Præbel[2], S. Bhat[2], S. -E. Fevolden[1], J. S. Christiansen[1]

[1]Department of Arctic and Marine Biology, UiT The Arctic University of Norway, 9037 Tromsø, Norway
[2]Norwegian College of Fishery Science, UiT The Arctic University of Norway, 9037 Tromsø, Norway

ABSTRACT: The starry ray *Amblyraja radiata* (Donovan, 1808) is widely distributed in the North Atlantic Ocean. Although considered a single species, there is large variation in size-at-maturity in the NW Atlantic, and Red List status ranges from 'Least Concern' in the NE Atlantic via 'Vulnerable' in Canadian waters to 'Critically Endangered' in US waters. Previous studies have documented regional morphological, morphometric, and ecological differences, without giving any conclusive evidence on reproductive isolation. Here, we use 10 microsatellite loci and 656 specimens originating from waters off northern Canada, eastern and western Greenland, Svalbard, the Barents Sea, the Norwegian Sea, and the North Sea, to (1) elucidate the population genetic structure of *A. radiata,* and (2) clarify whether differences in life history within the NW Atlantic is correlated to genetic structuring. The results suggested that *A. radiata* within the North Atlantic may be divided into 3 major clusters that coincide with the geographical regions NW Atlantic, Greenland and NE Atlantic. However, large physical mixing of individuals from different populations and with differentiated life histories throughout the North Atlantic suggested that glacial periods and biological features have shaped the contemporary distribution and genetic signatures of *A. radiata*. The differentiated life histories within the NW Atlantic specimens cannot be attributed to a genetic component, based on the present data.

KEY WORDS: Thorny skate · Rajidae · Cryptic · Phenotypic plasticity

INTRODUCTION

The starry ray *Amblyraja radiata* occupies a wide range of seas, temperatures and depths. In the NW Atlantic it is found from South Carolina in the south (Bigelow & Schroeder 1953) to Baffin Bay in the north (Coad & Reist 2004), and throughout most of the Greenlandic shelf (Møller et al. 2010). In the NE Atlantic, it occurs from the Dutch coast to Iceland, Norway and Svalbard Archipelago (Bigelow & Schroeder 1953), to Novaya Zemlya in the east (Wienerroither et al. 2011a).

Originally, the species was described by Donovan (1808) on the basis of a single specimen caught in the 'north ocean of Britain'. Garman (1913) concluded that due to the larger size, less roughness and 'rather more angular' appearance, the NW Atlantic population should be named *Raia scabrata*. Andriyashev (1964) noticed a spine between the dorsal fins as a characteristic of *R. scabrata*, but doubted its validity as a separate species. Bigelow & Schroeder (1953) did not find any morphological differences that justified 2 species, except high variation in size-at-maturity. Consequently, they merged the 2 species into one, which is now recognised as *Amblyraja radiata* (Donovan, 1808)

A. radiata is the most abundant skate species in the Barents Sea (Dolgov et al. 2005a) and in the North

*Corresponding author: arve.lynghammar@uit.no

Sea (Skjæraasen & Bergstad 2000), where it represents ~90% of the skate biomass. There are no targeted fisheries for the species in either the North Sea or the Barents Sea (Walker & Heessen 1996, Dolgov et al. 2005b), but landings from the Icelandic fisheries have increased since the 1990s. There is a market demand for skates in Iceland, where the common skate complex *Dipturus batis* is replaced by *A. radiata* because the former has become rare (Icelandic Fisheries 2014). In the Canadian Atlantic, *A. radiata* is commercially targeted on the Grand Banks (COSEWIC 2012). Although the abundance of *A. radiata* has increased in the North Sea (Walker & Heessen 1996), it has declined in some regions in the NW Atlantic (e.g. Swain et al. 2005, McPhie & Campana 2009, COSEWIC 2012), probably because of fishery pressure and predation by grey seal *Halichoerus grypus* (Swain et al. 2013). Consequently, the conservation status of *A. radiata* varies across its geographical range, and the International Union for Conservation of Nature (www.iucnredlist.org) categorises the species as 'Least Concern' in the NE Atlantic, 'Vulnerable' in Canadian waters, and 'Critically Endangered' in US waters (Kulka et al. 2009).

The extent of gene flow across the Atlantic may be low for *A. radiata* and other skates, as tagging studies have revealed small home ranges. A 20 yr tagging study of 722 *A. radiata* in the Newfoundland area suggested that the species is stationary, and most recaptures occurred within ~100 km and no farther than 444 km from the release site (Templeman 1984a). Walker et al. (1997) tagged skates in the North Sea, and among them 159 *A. radiata*. Most recaptures (85%) were done within 93 km (max. 180 km) of the release site. Small-eyed ray *Raja microocellata,* blonde ray *R. brachyura* and undulate ray *R. undulata* tagged in the English Channel were usually recaptured within 20 km (max. 61 km) of the release site (Ellis et al. 2011). A total of 18180 big skate *R. binoculata* were tagged off the western coast of Canada and 75% of the recapture was within 21 km of the release site (King & McFarlane 2010). In other words, skates appear highly philopatric and do not undertake long distance migrations.

In general, larger marine fishes tend to migrate further than smaller (Roff 1988). Life history and reproductive mode does matter, with broadcast spawning and planktonic development being important factors for long distance migration potential (Goodwin et al. 2005). Egg-laying teleosts tend to have a wider latitudinal range (i.e. distribution) than live-bearers, whereas the opposite seems true for elasmobranchs (Goodwin et al. 2005). According to this theory, *A. radiata*, being an egg-laying elasmobranch, has low potential for dispersal. Further, it is thought to be an obligate bottom-dweller at down to 1000 m depth (Stehmann & Burkel 1984). The deeper parts of the NE Atlantic may thus impede dispersal. The sill depth in the Fram Strait is approximately 2600 m, with deeper waters both in the Arctic Ocean to the north and the Greenland Sea to the south (Blindheim 2004). With the exception of some studies on hydrothermal vents at the Kolbeinsey Ridge (Fricke et al. 1989) and Mohn Ridge (Schander et al. 2010), the diversity of fishes in the northern part of the Mid-Atlantic Ridge is poorly investigated. A review of the Jan Mayen Island fishes did not reveal any records of *A. radiata* (Wienerroither et al. 2011b). Dispersal along these ridges cannot be excluded, but these are less likely compared to the route along the Norwegian continental shelf. The maximum sill depth between Scotland and Greenland is 840 m (Blindheim 2004) and seems a likely dispersal route for *A. radiata* within the NE Atlantic. Dispersal may also occur between Greenland and Canada via the Greenland-Canada ridge where the sill depth is <700 m (Jørgensen et al. 2005), or via the northern part of Baffin Bay (Jørgensen et al. 2011). Nevertheless, despite low dispersal potentials *A. radiata* is the second most widely distributed chondrichthyan north of the North Atlantic (as defined by the International Hydrographic Organization, www.iho.int), only surpassed by the Greenland shark *Somniosus microcephalus* (Lynghammar et al. 2013).

Cryptic species are 2 or more distinct species that are erroneously classified under one species name, and the discovery of such species has increased exponentially after the introduction of molecular techniques (Bickford et al. 2007, Pfenninger & Schwenk 2007, Portnoy & Heist 2012). If an examination indicates consistent difference (i.e. genetics, morphology) leading to reproductive isolation, splitting into separate species may be considered. Following genetic screening, morphological differences are often revealed, such as in the common skate complex *Dipturus batis*, where e.g. size-at-maturity of the 2 species are so different that mating is physically impossible (Iglésias et al. 2010). Cryptic species are almost evenly distributed across major metazoan taxa and geographical regions when correcting for species richness and study intensity (Pfenninger & Schwenk 2007).

Pronounced variations in meristics and life histories for *A. radiata* across the North Atlantic suggest population structuring and probably also cryptic speciation. Off the Canadian east coast, Templeman

(1984b) found a north–south latitudinal cline in the number of median dorsal thorns and tooth rows, and corresponding meristics from Icelandic specimens showed intermediate values between northern and southern specimens. More striking differences relate to size-at-maturity and maximum total length (TL), as *A. radiata* displays 2 contrasting life histories. In the NW Atlantic, individuals off Baffin Island and the Labrador shelf mature at about 440 to 500 mm (max. 720 mm) TL, whereas those further south, on the Grand Bank and St. Pierre Banks, mature at about 650 to 680 mm (max. 1040 mm) TL (Templeman 1987). COSEWIC (2012) recognises latitude 49°N as the boundary between the southern (large) and northern (small) *A. radiata*. Moreover, the abundance of *A. radiata* peaks within temperature ranges 1 to 3°C and 6 to 9°C to the south and at 1 to 3°C to the north. This is also an indication of discrete populations, but COSEWIC (2012) does not include any size-at-maturity data and it is therefore not possible to relate temperature to life history. In the North Sea and Skagerrak, *A. radiata* mature at about 440 mm (max. 720 mm) TL (Skjæraasen & Bergstad 2000) which is similar to the northern *A. radiata* in the NW Atlantic. Maximum TL in skates is positively correlated with size-at-maturity (Templeman 1987, Iglésias et al. 2010, Kelly & Hanson 2013), and a maximum TL of 750 mm in the Barents Sea (Dolgov et al. 2005a) implies a relatively small size-at-maturity also in this region. In other words, size-at-maturity in the NE Atlantic resembles that of the northern NW Atlantic (see Table 1 for regional and sexual differences regarding size-at-maturity and maximum TL).

A remarkably high number of haplotypes is found in *A. radiata* using a single genetic marker (Chevolot et al. 2007, Coulson et al. 2011, Lynghammar et al. 2014), raising the possibility of cryptic species or at least pronounced population structuring. In addition to Templeman's (1987) observed geographical variation in size-at-maturity, Sosebee (2005) and McPhie & Campana (2009) found bimodal size distribution of mature specimens, further indicating cryptic speciation in the NW Atlantic. The objectives of the present study were to test the hypotheses that (1) *A. radiata* in the NW Atlantic, Greenland and the NE Atlantic are genetically segregated due to low migration potential and (2) there is genetic differentiation between the early and late maturing individuals in the NW Atlantic.

MATERIALS AND METHODS

Specimens of *Amblyraja radiata* (N = 656) were sampled from research and commercial vessels across the North Atlantic (Fig. 1). Muscle or fin tissues were taken from fresh or frozen specimens and stored in 96% ethanol at −20°C until DNA extraction. The specimens were divided into groups of samples (hereafter 'samples') according to geographical locality or size-at-maturity; see Fig. 1 for location abbreviations. NW Atlantic *A. radiata* are hereafter termed

Table 1. *Amblyraja radiata*. Size-at-maturity and maximum total lengths (mm) for males (M) and females (F) from the literature. Size-at-maturity without denotation refer to the smallest mature specimens, while calculated lengths at 50% maturity are denoted L_{50}. Note that maturity status may be defined differently among authors

Region	Size-at-maturity	Max. size	Reference
Baffin Island and Labrador Shelf, W Greenland and N Iceland	M: 440–500 (L_{50}) F: 440–470 (L_{50})	M: 700–720 F: 610–630	Templeman (1987)
Grand Bank, St. Pierre Bank and vicinity	M: 680–830 (L_{50}) F: 650–740 (L_{50})	M: 1040 F: 940	Templeman (1987)
Eastern Scotian Shelf	M: 626 (L_{50}) F: 534 (L_{50})	M: ~920 F: ~850	McPhie & Campana (2009)
Western Gulf of Maine	M: 800 F: 820	M: 1040 F: 1050	Sulikowski et al. (2005)
Western Gulf of Maine	M: 870 (L_{50}) F: 873 (L_{50})	M: 1003 F: 1005	Sulikowski et al. (2006)
Gulf of Maine	M: 500 (but high variation) F: 430–460	M: ~1020 F: ~980	Sosebee (2005)
North Sea and Skagerrak	M: 440 (L_{50}) F: 440 (L_{50})	M: 720 F: 720	Skjæraasen & Bergstad (2000)
Barents Sea		M & F: 750	Dolgov et al. (2005a)

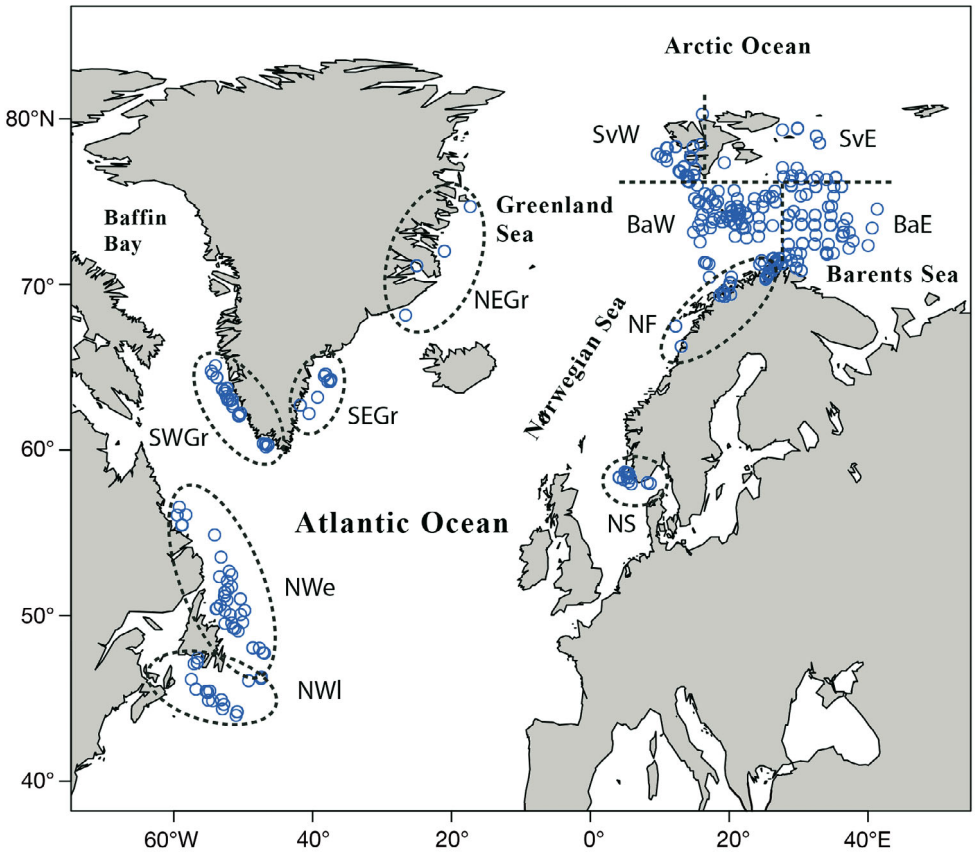

Fig. 1. *Amblyraja radiata*. Distribution of samples throughout the North Atlantic. One data point may comprise several specimens. Samples were collected from the following locations: northwest Atlantic late maturing (NWl), northwest Atlantic early maturing (NWe), southwest Greenland (SWGr), southeast Greenland (SEGr), northeast Greenland (NEGr), Svalbard west (SvW), Svalbard east (SvE), Barents Sea west (BaW), Barents Sea east (BaE), Norwegian fjords (NF) and the North Sea (NS). Map drawn in the software R (R Core Team 2014)

as 'late' (NWl) or 'early' (NWe) maturing, assuming that size and age are positively correlated. Males were categorised as early or late maturing based on the relationship between TL and clasper length, whereas females were internally examined to determine maturation stage versus TL (C. Miri, Fisheries and Oceans Canada, pers. comm.).

Microsatellite analyses

Fourteen microsatellite loci were amplified via the polymerase chain reaction (PCR) using forward (labelled) and reverse primers arranged into 3 PCR-multiplexes (see Table S1 in the Supplement at www.int-res.com/articles/suppl/m562p123_supp.pdf). The reactions consisted of 1.50 µl Type-it® Microsatellite Master Mix (Qiagen), 0.25 µl primer mix, (concentration range from 0.25 to 0.40 µM), 0.25 µl ultra-pure H_2O, and 0.50 µl DNA template, to a total volume of 2.50 µl. The PCR cycles consisted of an initial denaturing step at 95°C for 15 min, followed by 25 cycles at 94°C for 30 s, 57°C for 3 min and 72°C for 1 min, with a final extension step at 60°C for 30 min. The PCR products were separated on an ABI 3130XL automated genetic analyser using LIZ-500 as internal size-standard. The alleles were scored using predefined bins in Genemapper 3.7 (Applied Biosystems), and verified by manual inspection.

Data analysis

The samples were screened for null alleles and scoring errors in the software MICRO-CHECKER 2.2.3 (Van Oosterhout et al. 2004), using 1000 bootstrap replications to generate the expected homozygote and heterozygote allele frequencies. The within sample genetic variation indices: number of alleles (N_A); expected (H_e) and observed (H_o) heterozygosity; and the coefficient of inbreeding (F_{IS}) were estimated in GENEPOP 4.0 (Rousset 2008). Deviations from Hardy-Weinberg equilibrium (HWE) across all samples and loci and for each sample, linkage disequilibrium (LD) among loci over all samples, as well as the overall genetic differentiation within the dataset were tested by exact tests (Guo & Thompson 1992) using GENEPOP 4.0 (Rousset 2008). The pairwise p-values from the HWE and LD tests were corrected for multiple comparisons by sequential Bon-

Table 2. *Amblyraja radiata*. Pairwise F_{ST} values (Weir & Cockerham 1984) between sampling locations. See Fig. 1 legend for location abbreviations. $^{*}p < 0.05$, $^{**}p < 0.01$

	SvW	SvE	BaE	BaW	NF	NS	NEGr	SEGr	SWGr	NWe
SvE	−0.003									
BaE	−0.001	−0.003								
BaW	0.001	−0.003	0.001							
NF	0.001	−0.004	0.000	0.000						
NS	0.010	−0.003	0.003	0.009	0.010					
NEGr	0.032	0.040*	0.034*	0.021	0.027	0.066*				
SEGr	0.001	−0.005	−0.004	0.002	−0.002	−0.008	0.032			
SWGr	0.010*	0.002	0.009*	0.005*	−0.001	0.016*	0.020	0.003		
NWe	0.068**	0.069**	0.068**	0.060**	0.053**	0.085**	0.021	0.072**	0.047**	
NWl	0.090**	0.089**	0.087**	0.079*	0.068**	0.100**	0.051*	0.085**	0.067**	0.004

ferroni corrections (SBC) following Rice (1989). Allelic (Ar) and private allelic richness (pAr) per sample were estimated, accounting for differences in sample sizes, using the rarefaction procedure for the smallest sample size (40 genes) as implemented in the software HP-RARE 1.0 (Kalinowski 2005).

Genetic differentiation among samples was estimated via pairwise F_{ST} values (Weir & Cockerham 1984) in Arlequin 3.5 (Excoffier et al. 2007), and tested for statistical significance using 10 000 permutations (Table 2). The spatial structures as revealed by F_{ST} were visualized in a neighbour-joining (NJ) tree using 1000 permutations to estimate robustness of branching. The tree was constructed and branching was tested for robustness using the online version of POPTREE2 (Takezaki et al. 2010), POPTREEVIEW (www.med.kagawa-u.ac.jp/~genomelb/takezaki/poptreew/). To infer whether the spatial structure among samples was driven by isolation by distance, i.e. when nearest neighbours are more genetically similar than more distant neighbours, or the population structure is driven by e.g. barriers to gene flow or biological factors, the pairwise F_{ST} values were transformed into Rousset's distance, i.e. $F_{ST}/(1 - F_{ST})$, and correlated to geographical distance. The correlation was tested for significance using isolation by distance (IBD; Bohonak 2002) with 10 000 permutations. All negative pairwise F_{ST} estimates were changed to 0.00001. Geographical distances between pairs of samples were estimated using the Daft Logic Distance Calculator (www.daftlogic.com/projects-google-maps-distance-calculator.htm). Log-transforming the genetic and/or the geographical distance did not change the result of this test.

To avoid the bias of *a priori* geographical grouping of individuals and obtain estimates of the proportion of admixture and physical mixture among individuals within geographical locations, a Bayesian clustering method was used as implemented in STRUCTURE 2.3.3 (Pritchard et al. 2000, Hubisz et al. 2009). A modified dataset was used for these analyses, where the number of individuals from the Barents Sea (locations BaE and BaW) was randomly reduced to 63 and 55, respectively, to minimize the effect of large sample sizes on the allele frequency distributions, i.e. HWE and LD, used by the model. Due to the high connectivity in marine systems (Ward et al. 1994), we used a model that assumed admixture and correlated allele frequencies between K clusters. To determine the appropriate number of burn-ins and Markov chain Monte Carlo (MCMC) replications needed for the model to converge, we tested burn-ins and MCMC replications in the ranges 50 000 to 300 000 and 100 000 to 500 000, respectively, at several values of K. After evaluating the summary statistics for each K-value, we chose to use varying burn-ins of 100 000 and 200 000 replications and 200 000 to 300 000 MCMC replications for the analyses. The model was run a minimum of 5 times at each K-value to confirm consistency of log-likelihood probabilities. No additional prior information was provided for the model. The most likely highest ln $\Pr(X|K)/\Delta K$ (Evanno et al. 2005) grouping was found using STRUCTURE HARVESTER (Earl & vonHoldt 2012). High levels of physical mixture of individuals within samples and among the inferred clusters were observed in the initial runs and the analyses therefore adopted a hierarchical approach (Vähä et al. 2007), focusing only on clustering inference from ΔK. The evaluation of the first hierarchical level ($K = 1$ to 15) used a conservative evaluation of the proportion of membership of each individual in each of the K clusters, using q value thresholds of 0.3 and 0.7 (Vähä & Primmer 2006, Vähä et al. 2007, Warnock et al. 2010). For the consecutive runs of deeper hierarchi-

Table 3. *Amblyraja radiata*. Names and abbreviations of sample locations, geographical centres of samples (given in decimal degrees), number of individuals (N) included in each sample (for the full data set), and results of statistical analysis. Ar: allelic richness; pAR: private allelic richness; H_e: expected heterozygosity; H_o: observed heterozygosity; F_{IS}: Wright coefficient of inbreeding. Significant departures from Hardy-Weinberg equilibrium (HWE) are indicated as bold F_{IS} values. The NEGr sample was excluded in the estimates of Ar and pAr due to small sample size

Location	Sample location	Location abbreviation	N	Ar	pAr	H_o	H_e	F_{IS}
Svalbard west	78.0° N, 11.2° E	SvW	69	5.2	0.09	0.553	0.557	0.008
Svalbard east	78.8° N, 27.44° E	SvE	30	5.4	0.09	0.585	0.576	0.017
Barents Sea east	74.4° N, 32.2° E	BaE	189	5.4	0.09	0.565	0.577	0.020
Barents Sea west	74.5° N, 20.6° E	BaW	141	5.2	0.05	0.563	0.581	0.032
Norwegian fjords	70.0° N, 18.0° E	NF	45	5.3	0.06	0.598	0.592	0.010
North Sea	58.3° N, 5.8° E	NS	23	5.9	0.42	0.507	0.550	0.079
Northeast Greenland	72.7° N, 21.0° W	NEGr	5	–	–	0.511	0.603	0.153
Southeast Greenland	64.1° N, 39.4° W	SEGr	21	6.3	0.54	0.576	0.566	0.017
Southwest Greenland	64.1° N, 52.6° W	SWGr	62	5.5	0.12	0.597	0.597	0.001
NW Atlantic early maturing	51.2° N, 53.4° W	NWe	43	5.7	0.25	0.616	0.635	**0.032**
NW Atlantic late maturing	45.2° N, 56.4° W	NWl	28	5.4	0.18	0.620	0.604	**–0.026**

cal levels a stricter threshold value of q (0.2 and 0.8) was used. For each hierarchical level, the individuals inferred in each of the K clusters were identified and the relative contribution of each geographical locality estimated. The analyses were terminated at the second hierarchical level, as the number of individuals within each cluster at this point was too low to provide any statistical support for further analyses.

To complement the STRUCTURE analyses, we performed a discriminant analysis of principal components (DAPC) using the R package *adegenet* (Jombart et al. 2010). DAPC is a non-model-based method that describes the diversity between predefined groups of observations as best as possible, while minimising the within-group variation. To investigate the number of clusters in the dataset, we used the *find.clusters* function employed in *adegenet* using Bayesian information criterion (BIC) and retained all the principal components (PCs). The DAPC analysis was performed using function *dapc.* DAPC relies on data transformation using principal component analysis (PCA) as a prior step. Retaining too many PCs will lead to an overfitting of discriminant functions and result in discrimination of any sets of the clusters. To avoid this bias, we determined the optimum number of PCs to be retained for the DAPC analysis as 13, by the *optim.a.score* method (Jombart et al. 2010). As the number of expected clusters was small we selected all the discriminant functions. To obtain a visual assessment of between-population differentiation, we used location as a prior in the DAPC analysis by retaining PCs that explained ~85% of total observed variance.

RESULTS

Four (Ar-132, Ar-149, Ar-9m13, and LERI-63) out of the original 14 loci were indicated as influenced by null alleles or other locus/PCR abnormalities and were therefore omitted from further analyses. Summary statistics for the remaining 10 microsatellite loci are listed in Table S2 in the Supplement. Number of alleles per locus ranged from 2 at locus Ar-20 to 11 at loci Ar-130 and LERI-44. Nine out of 110 loci per sample showed departure from HWE, but none of the comparisons were significant after SBC at the $p < 0.05$ level. Six out of 45 pairwise locus comparisons were significant for LD, but the combinations were randomly distributed among 6 loci and all samples.

Total number of alleles across loci per sample varied from 59 in NWl, (37 in NEGr, but only 5 individuals were available) to 74 in BaE (Table S2), with an average across samples of 62. The allelic (Ar = 5.2 ± 0.6 to 6.3 ± 0.7) and private allelic (pAr = 0.05 ± 0.02 to 0.54 ± 0.14) richness and expected heterozygosity (H_e = 0.550 to 0.635) did not reveal any distinct geographical patterns (Table 3). However, SEGr displayed higher allelic and private allelic richness, but similar or lower H_e than the other samples. Two samples (NWe and NWl) of the 11 tested showed significant departures from the HWE-expectations associated with both heterozygote deficit and excess, respectively (Table 3).

The exact test for genetic structure was highly significant (χ^2 = infinity, df = 20, $p < 0.001$) across all samples and together with a highly significant HWE test across all loci and samples (indicating a sample of mixed populations), suggests the existence of population structure among samples.

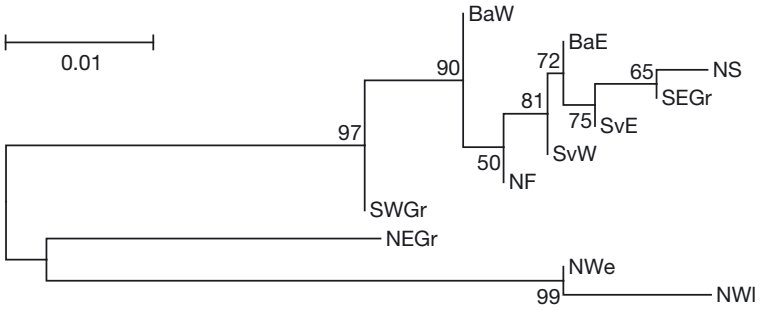

Fig. 2. *Amblyraja radiata*. Neighbour-joining tree of samples collected from different locations in the North Atlantic, using corrected F_{ST} distances. Numbers at the nodes are bootstrap values (1000 iterations). See Table 3 for location abbreviations

The global genetic differentiation was estimated to be F_{ST} = 0.019, and significant pairwise F_{ST} values among samples varied from 0.009 (SWGr vs. BaE) to 0.100 (NWl vs. NS) (Table 2). The samples from the NW Atlantic were significantly differentiated from all other samples except NEGr (Table 2, Fig. 2), suggesting population structuring between the NW Atlantic and the NE Atlantic. It should be noted that the sample of NEGr only contained 5 individuals and the results related to this sample should therefore be treated with caution. Samples from within the NE Atlantic did not display any particular patterns of F_{ST} (Table 2), which is also supported by the NJ tree (Fig. 2). SWGr displayed F_{ST} values significantly different from samples from the Barents Sea (BaE and BaW), SvW and NS. Thus, the pairwise F_{ST} values suggest 3 genetically differentiated and geographically separated groups of individuals: the NW Atlantic, Greenland, and the NE Atlantic. However, this pattern was not clearly supported by the NJ tree. The samples from the NW Atlantic representing individuals with differentiated life histories (NWe and NWl) were associated with a low (F_{ST} = 0.004) and non-significant pairwise F_{ST} estimate.

There appear to be other factors than geographical distance that influence the structuring among the samples as the correlations of pairwise estimates of Rousset's distance and geographical distance were non-significant (Mantel test; Z = 3312, r = −0.1566, p = 0.9). This result is supported by the Bayesian clustering analyses that revealed a large proportion of physical mixture among spatial sampling locations (Fig. 3A). The first round of STRUCTURE analysis clustered the individuals into 2 clusters (ΔK = 2) containing 159 and 158 individuals and left 127 individuals unassigned (Fig. 3B). The first round of clustering assigned mainly NE Atlantic individuals into Cluster 1 (R1A) whereas Cluster 2 (R1B) contained a high proportion of the NW Atlantic individuals, but also a proportion of NE Atlantic and Greenland individuals (Fig. 3C). The unassigned individuals from the first round of STRUCTURE analysis were composed of nearly random sample locations (R1Un, Fig. 3C). The consecutive STRUCTURE runs (Runs 2 to 4) of the R1A, R1B and R1Un, further structured the individuals into 7 clusters, leaving a total of 156 individuals unassigned among the 7 clusters (Fig. 3D). The R1A was divided into 2 (ΔK = 2) additional clusters (R2A and R2B) with approximately equal proportions of NE and Greenland individuals assigned to them (Fig. 3E). The R1B cluster was divided into 3 (ΔK = 3) additional clusters (R3A, R3B, and R3C). R3A consisted of individuals from all regions, except BaE, SvE and NEGr. R3B solely contained NW Atlantic and a low proportion of SEGr individuals. The third cluster (R3C) was composed only of individuals from the NE and Greenland, whereas the unassigned individuals from this run (R3Un) originated from all sample locations. The final run was to resolve the R1Un, and revealed 2 (ΔK = 2) additional clusters (R4A and R4B), composed of individuals from all sample locations except NEGr.

The DAPC analysis using the *find.cluster* function showed an ambiguous number of clusters (Fig. S1 in the Supplement), as revealed by the probable number between 10 and 20. The frequency plot for the inferred groups (K = 11, which is number of sample locations), suggested no clear pattern in retrieval of the original sample locations. The exceptions were NWe and NWl, where the sample locations appeared to contribute to the inferred clusters (Fig. S2). The DAPC scatter plot, where we used the sampling location as prior, showed that the first axis slightly separates NWe and NWl, with substantial overlapping between their respective inertia eclipses (Fig. S3 in the Supplement), while the second axis of DA separates NWe and NWl from the remaining sample locations, but still with a clear overlap of inertia ellipses.

DISCUSSION

Population genetic structure

Oceanic features, such as current patterns, temperature clines and bathymetry, and the physiological capacity of fishes (e.g. swimming performance and ther-

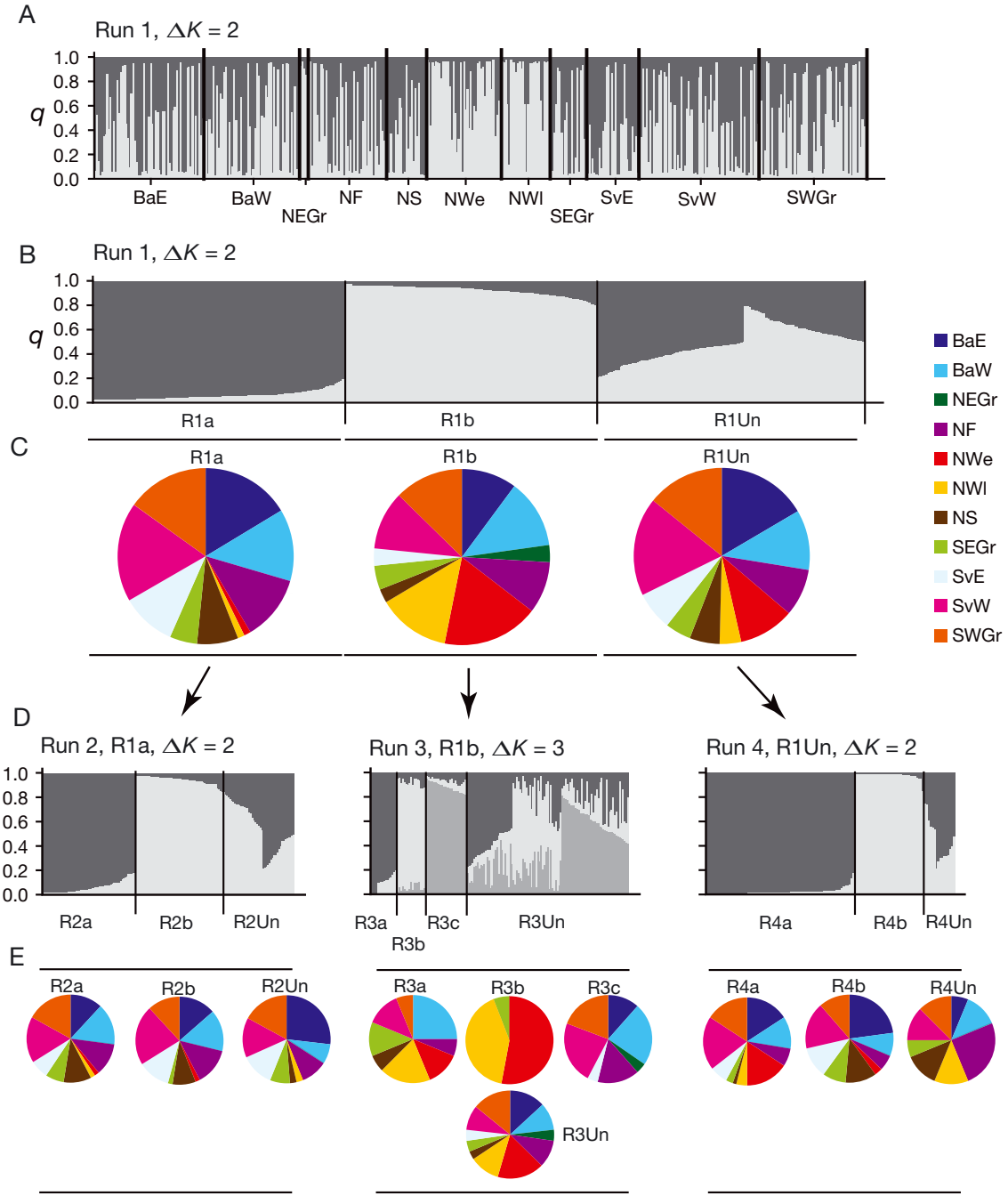

Fig. 3. *Amblyraja radiata*. Population structuring among the 11 samples (N = 444) using 2 rounds of hierarchical STRUCTURE analysis. Each individual is represented by a thin vertical line, which is partitioned into *K*-coloured segments representing the individual's estimated membership fractions (*q*) in Δ*K* clusters (Evanno et al. 2005). The first round of STRUCTURE analysis revealed that the individuals were partitioned into 2 clusters (Δ*K* = 2) and are here given as (A) sorted by spatial sample locations (separated by thick black lines) and (B) sorted by an individual's estimated membership (*q*) to a cluster, given the *q*-value thresholds of 0.3 and 0.7. Using the *q*-value thresholds to assign the membership of an individual to each of the 2 inferred clusters (R1a, R1b) left some of the individuals unassigned (R1Un). The relative proportion of individuals from each of the spatial sample locations in each of these clusters is given in (C). The 2 inferred clusters and the unassigned individuals were included in the second round (Runs 2 to 4) of STRUCTURE analyses, where the *q*-value thresholds for an individual's membership to a given cluster were increased to 0.2 and 0.8 (D). The identified clusters for these 3 STRUCTURE runs are labelled R2a–b, R3a–c and R4a–b. The relative proportions of individuals from each sample in each of the inferred clusters are given in (E). Colour key: Barents Sea east (BaE), Barents Sea west (BaW), Northeast Greenland (NEGr), Norwegian fjords (NF), Northwest Atlantic early maturing (NWe), Northwest Atlantic late maturing (NWl), the North Sea (NS), Southeast Greenland (SEGr), Svalbard east (SvE), Svalbard west (SvW) and Southwest Greenland (SWGr)

mohaline tolerance) are well-known factors contributing to population genetic structuring of marine fishes (e.g. Knutsen et al. 2009, Lamichhaney et al. 2012, Teacher et al. 2013). Genetic evidence for structuring of marine species over large spatial scales is starting to accumulate. Most studies have focused on economically important species, such as Atlantic cod *Gadus morhua* (Bradbury et al. 2010, Hemmer-Hansen et al. 2014), Atlantic herring *Clupea harengus* (André et al. 2011) and capelin *Mallotus villosus* (Dodson et al. 2007, Præbel et al. 2008), that mostly share the common feature of being highly mobile and undertake substantial spawning migrations. Such features, along with massive population sizes, weaken population structure at neutral loci, since the neutral genomic regions flow freely among populations.

Amblyraja radiata is a benthic, largely resident, low fecund fish species with no planktonic life stage and, considering the life history characteristics, some of the results herein are intriguing to interpret. Although the genetic structure of sharks has received considerable attention (e.g. Heist et al. 1996, Feldheim et al. 2001, Vignaud et al. 2014), similar studies on skates are now catching up (Chevolot et al. 2006, Griffiths et al. 2010, 2011, Pasolini et al. 2011, Ball et al. 2016). By analysing the mitochondrial cytochrome *c* gene for parts of the material used in the present study, Lynghammar et al. (2014) found significant pairwise F_{ST} values between the NE Atlantic and NWe, and between the NE Atlantic and NWl of 0.066 and 0.133, respectively, with a global F_{ST} of 0.070. However, Greenland samples were not significantly different from either the NE Atlantic or the NW Atlantic. Chevolot et al. (2007) sampled *A. radiata* from its southern distributional range, including Iceland. Using variation at the mitochondrial cytochrome *b* gene, a global θ = 0.019 (analogous to F_{ST}) was found, which corresponds to the level of differentiation estimated in the present study. However, when Chevolot et al. (2007) removed the Kattegat samples (which are close to our NS samples), the significant signal was lost. Interestingly, with the exception of the above mentioned Kattegat samples, the Newfoundland samples (which were sampled between our NWe and NWl sites) of Chevolot et al. (2007) were not significantly differentiated from any of the other locations when compared pairwise. In contrast, significant high genetic structuring within 3 regions (global θ = 0.042 and 0.348 for microsatellites and mitochondrial DNA, respectively), and significant isolation by distance, were found in another European skate, the thornback ray *Raja clavata* (Chevolot et al. 2006).

The present study examines the population genetic structure in *A. radiata*, and whether there is a genetic component in the differentiated life histories (i.e. early and late maturation). The results revealed a high proportion of physical mixing of individuals over large spatial scales, but also that fine scaled structure of individuals may be present within the North Atlantic. Importantly, the results suggest that *A. radiata* may be divided into 3 major clusters in the North Atlantic Ocean comprising the NE Atlantic, Greenland and the NW Atlantic.

Although the pairwise F_{ST} distances (Table 2) were biologically meaningful, the IBD was not significant. The results from STRUCTURE (Fig. 3) and the DAPC (Fig. S3 in the Supplement) indicated a high proportion of physical mixing of individuals throughout the North Atlantic Ocean, suggesting that this species may undertake long distance migrations. To infer whether this result is also concordant with analysis of mtDNA, we identified 60 individuals assigned to the clusters R1a, R1b, and R1Un (Fig. 3B) that were also included in Lynghammar et al. (2014) and used these 60 individuals to create a composite haplotype network (Fig. S4 in the Supplement). This haplotype network supported the fact that structuring is based on genotype rather than geographical location. However, long-distance migration is inconsistent with the results of tagging experiments (Templeman 1984a, Walker et al. 1997), and the apparent physical mixing of individuals may originate from periods of glacial expansions and retreats. In such a situation, populations from different geographical areas may have shared a common refuge where reproductive isolation mechanisms, such as assortative mating, may have preserved a clear genetic signature among populations. In post-glacial times the individuals may then have colonised the North Atlantic randomly and preserved their previous population signatures via assortative mating. Whether this scenario is valid remains to be shown. However, our results also suggest that further substructure may be present throughout the distributional range, which may support this scenario.

Life history variation

The marked differences in size-at-maturity and maximum size (Table 1) between the 2 samples from the NW Atlantic, would suggest reproductive isolation, but this is not supported by our genetic analyses. Large variation in life history traits has also been found in winter skate *Leucoraja ocellata*: earlier maturation and smaller maximum lengths were charac-

teristic for the southern Gulf of St. Lawrence individuals and, although no genetic methods were applied, splitting of the *L. ocellata* has been suggested (Kelly & Hanson 2013). Based on the data obtained insofar, and supported by data from barcoding (Lynghammar et al. 2014), splitting of *A. radiata* is not recommended. However, it should be noted that the present study used alleged neutral loci, which are not suited to reveal the early steps of speciation. When a reproductive isolation evolves in sympatry (in the presence of gene flow, referred to as ecological speciation; Coyne & Orr 2004), it involves an intricate balance where genomic and phenotypic divergence accumulate on the one side as a result of divergent neutral selection, and face the homogenising effects of gene flow on the other side (Gavrilets & Vose 2005). At the initial stages of divergence under gene flow, adaptive genomic differences accumulate much more strongly than neutral differences, as gene flow homogenises neutral genomic regions and divergent selection leads to the emergence of adaptive genomic regions (fitness/adaptive islands). Later in the process, neutral genomic regions may also start to accumulate differentially, as reproductive isolation starts to build up (but see Coyne & Orr 2004, Feder et al. 2013). Thus, future studies of the apparent cryptic structure of *A. radiata* may benefit from adopting a next generation sequencing approach in order to obtain genome-wide coverage of both neutral and adaptive loci.

Population genetic structuring is imperative when assessing Red List status (www.iucnredlist.org), as unknown migration barriers may prevent individuals from repopulating depleted areas (Dudgeon et al. 2009). Taken together, the results of STRUCTURE and DAPC analyses show a high degree of physical mixing of individuals over large geographical scales. However, the analyses also suggest that a fine scaled structure of individuals may be present within the North Atlantic and also support the results of F_{ST} estimates and the NJ tree in a sub-division of the Atlantic samples. For the purposes of conservation, our results suggest that the 3 major clusters outlined herein (NW Atlantic, Greenland and NE Atlantic) should be managed separately. Finally, our results also support that the differentiated life histories of the NW Atlantic individuals (NWe and NWl) may not be attributed to a genetic component.

Acknowledgements. We thank those who were involved in sample collection: T. Vollen and colleagues from the Institute of Marine Research in Norway, C. Miri at Fisheries and Oceans Canada, J. Y. Poulsen from the University of Bergen, N. Chernova from the Russian Academy of Sciences in St. Petersburg, Russia and H. Fock from the Thünen Institute of Sea Fisheries in Germany. The NE Greenland samples were obtained by the TUNU-Programme, UiT The Arctic University of Norway (UiT). T. L. Hanebrekke (UiT), K. Østbye (HiHM), 3 anonymous reviewers and the responsible editor P. Borsa are thanked for valuable discussions and criticism of earlier versions of this paper.

LITERATURE CITED

André C, Larsson LC, Laikre L, Bekkevold D and others (2011) Detecting population structure in a high gene-flow species, Atlantic herring (*Clupea harengus*): direct, simultaneous evaluation of neutral vs putatively selected loci. Heredity 106:270–280

Andriyashev AP (1964) Fishes of the northern seas of the U.S.S.R. Israel Program for Scientific Translations, Jerusalem. (English translation of Ryby severnykh morey SSSR, Moscow-Leningrad, 1954)

Ball RE, Serra-Pereira B, Ellis J, Genner MJ and others (2016) Resolving taxonomic uncertainty in vulnerable elasmobranchs: Are the Madeira skate (*Raja maderensis*) and the thornback ray (*Raja clavata*) distinct species? Conserv Genet 17:565

Bickford D, Lohman DJ, Sodhi NS, Ng PKL and others (2007) Cryptic species as a window on diversity and conservation. Trends Ecol Evol 22:148–155

Bigelow HB, Schroeder WC (1953) Fishes of the western North Atlantic: sawfishes, guitarfishes, skates and rays. Sears Foundation for Marine Research, Yale University, New Haven, CT

Blindheim J (2004) Oceanography and climate. In: Skjoldal HR (ed) The Norwegian Sea ecosystem. Tapir Academic Press, Trondheim, p 65–96

Bohonak AJ (2002) IBD (Isolation By Distance): a program for analyses of isolation by distance. J Hered 93:153–154

Bradbury IR, Hubert S, Higgins B, Borza T and others (2010) Parallel adaptive evolution of Atlantic cod on both sides of the Atlantic Ocean in response to temperature. Proc R Soc B 277:3725–3734

Chevolot M, Hoarau G, Rijnsdorp AD, Stam WT, Olsen JL (2006) Phylogeography and population structure of thornback rays (*Raja clavata* L., Rajidae). Mol Ecol 15: 3693–3705

Chevolot M, Wolfs PHJ, Pálsson J, Rijnsdorp AD, Stam WT, Olsen JL (2007) Population structure and historical demography of the thorny skate (*Amblyraja radiata*) in the North Atlantic. Mar Biol 151:1275–1286

Coad BW, Reist JD (2004) Annotated list of the Arctic marine fishes of Canada. Can Manuscr Rep Fish Aquat Sci 2674

COSEWIC (2012) COSEWIC assessment and status report on the thorny skate *Amblyraja radiata* in Canada. Committee on the Status of Endangered Wildlife in Canada, Ottawa. http://publications.gc.ca/collections/collection_2013/ec/CW69-14-656-2012-eng.pdf (accessed 27 May 2016)

Coulson MW, Denti D, Van Guelpen L, Miri C, Kenchington E, Bentzen P (2011) DNA barcoding of Canada's skates. Mol Ecol Resour 11:968–978

Coyne JA, Orr HA (2004) Speciation. Sinauer Associates, Sunderland, MA

Dodson JJ, Tremblay S, Colombani F, Carscadden JE, Lecomte F (2007) Trans-Arctic dispersals and the evolu-

tion of a circumpolar marine fish species complex, the capelin (*Mallotus villosus*). Mol Ecol 16:5030–5043

Dolgov AV, Drevetnyak KV, Gusev EV (2005a) The status of skate stocks in the Barents Sea. J Northwest Atl Fish Sci 35:249–260

Dolgov AV, Grekov AA, Shestopal IP, Sokolov KM (2005b) By-catch of skates in trawl and long-line fisheries in the Barents Sea. J Northwest Atl Fish Sci 35:357–366

Donovan E (1808) The natural history of British fishes, including scientific and general descriptions of the most interesting species, and an extensive selection of accurately finished coloured plates, Vol 5. The author and F. C. and J. Rivington, London

Dudgeon CL, Broderick D, Ovenden JR (2009) IUCN classification zones concord with, but underestimate, the population structure of the zebra shark *Stegostoma fasciatum* in the Indo-West Pacific. Mol Ecol 18:248–261

Earl DA, vonHoldt BM (2012) STRUCTURE HARVESTER: a website and program for visualizing STRUCTURE output and implementing the Evanno method. Conserv Genet Resour 4:359–361

Ellis JR, Morel G, Burt G, Bossy S (2011) Preliminary observations on the life history and movements of skates (Rajidae) around the Island of Jersey, western English Channel. J Mar Biol Assoc UK 91:1185–1192

Evanno G, Regnaut S, Goudet J (2005) Detecting the number of clusters of individuals using the software STRUCTURE: a simulation study. Mol Ecol 14:2611–2620

Excoffier L, Laval G, Schneider S (2007) Arlequin (version 3.0): an integrated software package for population genetics data analysis. Evol Bioinform Online 1:47–50

Feder JL, Flaxman SM, Egan SP, Nosil P (2013) Hybridization and the build-up of genomic divergence during speciation. J Evol Biol 26:261–266

Feldheim KA, Gruber SH, Ashley MV (2001) Population genetic structure of the lemon shark (*Negaprion brevirostris*) in the western Atlantic: DNA microsatellite variation. Mol Ecol 10:295–303

Fricke H, Giere O, Stetter K, Alfredsson GA, Kristjansson JK, Stoffers P, Svavarsson J (1989) Hydrothermal vent communities at the shallow subpolar Mid-Atlantic ridge. Mar Biol 102:425–429

Garman S (1913) The Plagostomia (sharks, skates and rays). Harvard University, Museum of Comparative Zoology, Cambridge, MA

Gavrilets S, Vose A (2005) Dynamic patterns of adaptive radiation. Proc Natl Acad Sci USA 102:18040–18045

Goodwin NB, Dulvy NK, Reynolds JD (2005) Macroecology of live-bearing in fishes: latitudinal and depth range comparisons with egg-laying relatives. Oikos 110: 209–218

Griffiths AM, Sims DW, Cotterell SP, El Nagar A and others (2010) Molecular markers reveal spatially segregated cryptic species in a critically endangered fish, the common skate (*Dipturus batis*). Proc R Soc B 277:1497–1503

Griffiths A, Sims D, Johnson A, Lynghammar A, McHugh M, Bakken T, Genner M (2011) Levels of connectivity between longnose skate (*Dipturus oxyrinchus*) in the Mediterranean Sea and the north-eastern Atlantic Ocean. Conserv Genet 12:577–582

Guo SW, Thompson EA (1992) Performing the exact test of Hardy-Weinberg proportion for multiple alleles. Biometrics 48:361–372

Heist EJ, Musick JA, Graves JE (1996) Genetic population structure of the shortfin mako (*Isurus oxyrinchus*) inferred from restriction fragment length polymorphism analysis of mitochondrial DNA. Can J Fish Aquat Sci 53: 583–588

Hemmer-Hansen J, Therkildsen NO, Meldrup D, Nielsen EE (2014) Conserving marine biodiversity: insights from life-history trait candidate genes in Atlantic cod (*Gadus morhua*). Conserv Genet 15:213–228

Hubisz MJ, Falush D, Stephens M, Pritchard JK (2009) Inferring weak population structure with the assistance of sample group information. Mol Ecol Resour 9:1322–1332

Icelandic Fisheries (2014) Starry ray. www.fisheries.is/main-species/cartilaginous-fishes/starry-ray/ (accessed 10 Jun 2016)

Iglésias SP, Toulhoat L, Sellos DY (2010) Taxonomic confusion and market mislabelling of threatened skates: important consequences for their conservation status. Aquat Conserv 20:319–333

Jombart T, Devillard S, Balloux F (2010) Discriminant analysis of principal components: a new method for the analysis of genetically structured populations. BMC Genet 11:94

Jørgensen OA, Hvingel C, Møller PR, Treble MA (2005) Identification and mapping of bottom fish assemblages in Davis Strait and southern Baffin Bay. Can J Fish Aquat Sci 62:1833–1852

Jørgensen OA, Hvingel C, Treble MA (2011) Identification and mapping of bottom fish assemblages in northern Baffin Bay. J Northwest Atl Fish Sci 43:65–79

Kalinowski ST (2005) HP-RARE 1.0: a computer program for performing rarefaction on measures of allelic richness. Mol Ecol Notes 5:187–189

Kelly JT, Hanson JM (2013) Maturity, size at age and predator-prey relationships of winter skate *Leucoraja ocellata* in the southern Gulf of St Lawrence: potentially an undescribed endemic facing extirpation. J Fish Biol 82: 959–978

King JR, McFarlane GA (2010) Movement patterns and growth estimates of big skate (*Raja binoculata*) based on tag-recapture data. Fish Res 101:50–59

Knutsen H, Jorde PE, Sannæs H, Hoelzel AR and others (2009) Bathymetric barriers promoting genetic structure in the deepwater demersal fish tusk (*Brosme brosme*). Mol Ecol 18:3151–3162

Kulka DW, Sulikowski J, Gedamke J, Pasoloni P, Endicott M (2009) *Amblyraja radiata*. The IUCN Red List of Threatened Species 2009:e.T161542A5447511. http://dx.doi.org/10.2305/IUCN.UK.2009-2.RLTS.T161542A5447511.en (accessed 10 Jun 2016)

Lamichhaney S, Barrio AM, Rafati N, Sundström G and others (2012) Population-scale sequencing reveals genetic differentiation due to local adaptation in Atlantic herring. Proc Natl Acad Sci USA 109:19345–19350

Lynghammar A, Christiansen JS, Mecklenburg CW, Karamushko OV, Møller P, Gallucci VF (2013) Species richness and distribution of chondrichthyan fishes in the Arctic Ocean and adjacent seas. Biodiversity 14:57–66

Lynghammar A, Christiansen JS, Griffiths AM, Fevolden SE, Hop H, Bakken T (2014) DNA barcoding of the northern Northeast Atlantic skates (Chondrichthyes, Rajidae), with remarks on the widely distributed starry ray. Zool Scr 43:485–495

McPhie RP, Campana SE (2009) Reproductive characteristics and population decline of four species of skate (Rajidae) off the eastern coast of Canada. J Fish Biol 75: 223–246

Møller PR, Nielsen JG, Knudsen SW, Poulsen JY, Sünksen K, Jørgensen OA (2010) A checklist of the fish fauna of Greenland waters. Zootaxa 2378:1–84

Pasolini P, Ragazzini C, Zaccaro Z, Cariani A and others (2011) Quaternary geographical sibling speciation and population structuring in the Eastern Atlantic skates (suborder Rajoidea) *Raja clavata* and *R. straeleni.* Mar Biol 158:2173–2186

Pfenninger M, Schwenk K (2007) Cryptic animal species are homogeneously distributed among taxa and biogeographical regions. BMC Evol Biol 7:121

Portnoy DS, Heist EJ (2012) Molecular markers: progress and prospects for understanding reproductive ecology in elasmobranchs. J Fish Biol 80:1120–1140

Præbel K, Westgaard JI, Fevolden SE, Christiansen JS (2008) Circumpolar genetic population structure of capelin *Mallotus villosus.* Mar Ecol Prog Ser 360:189–199

Pritchard JK, Stephens M, Donnelly P (2000) Inference of population structure using multilocus genotype data. Genetics 155:945–959

R Core Team (2014) R: a language and environment for statistical computing. R Foundation for Statistical Computing, Vienna

Rice WR (1989) Analyzing tables of statistical tests. Evolution 43:223–225

Roff DA (1988) The evolution of migration and some life history parameters in marine fishes. Environ Biol Fishes 22: 133–146

Rousset F (2008) GENEPOP'007: a complete re-implementation of the GENEPOP software for Windows and Linux. Mol Ecol Resour 8:103–106

Schander C, Rapp HT, Kongsrud JA, Bakken T and others (2010) The fauna of hydrothermal vents on the Mohn Ridge (North Atlantic). Mar Biol Res 6:155–171

Skjæraasen JE, Bergstad OA (2000) Distribution and feeding ecology of *Raja radiata* in the northeastern North Sea and Skagerrak (Norwegian Deep). ICES J Mar Sci 57: 1249–1260

Sosebee KA (2005) Maturity of skates in Northeast United States waters. J Northwest Atl Fish Sci 35:141–153

Stehmann M, Burkel DL (1984) Gnathostomata. Rajidae. In: Whitehead PJP, Bauchot ML, Hureau JC, Nielsen J, Tortonese E (eds) Fishes of the north-eastern Atlantic and the Mediterranean. UNESCO, Paris, p 163–196

Sulikowski JA, Kneebone J, Elzey S, Jurek J, Danley PD, Howell WH, Tsang PCW (2005) The reproductive cycle of the thorny skate (*Amblyraja radiata*) in the western Gulf of Maine. Fish Bull 103:536–543

Sulikowski JA, Kneebone J, Elzey S, Jurek J, Howell WH, Tsang PCW (2006) Using the composite variables of reproductive morphology, histology and steroid hormones to determine age and size at sexual maturity for the thorny skate *Amblyraja radiata* in the western Gulf of Maine. J Fish Biol 69:1449–1465

Swain DP, Hurlbut T, Benoît HP (2005) Changes in the abundance and size of skates in the Southern Gulf of St. Lawrence, 1971–2002. J Northwest Atl Fish Sci 36:19–30

Swain DP, Jonsen ID, Simon JE, Davies TD (2013) Contrasting decadal trends in mortality between large and small individuals in skate populations in Atlantic Canada. Can J Fish Aquat Sci 70:74–89

Takezaki N, Nei M, Tamura K (2010) POPTREE2: software for constructing population trees from allele frequency data and computing other population statistics with windows interface. Mol Biol Evol 27:747–752

Teacher AGF, André C, Jonsson PR, Merilä J (2013) Oceanographic connectivity and environmental correlates of genetic structuring in Atlantic herring in the Baltic Sea. Evol Appl 6:549–567

Templeman W (1984a) Migrations of thorny skate, *Raja radiata*, tagged in the Newfoundland area. J Northwest Atl Fish Sci 5:55–63

Templeman W (1984b) Variations in numbers of median dorsal thorns and rows of teeth in thorny skate (*Raja radiata*) of the Northwest Atlantic. J Northwest Atl Fish Sci 5: 171–179

Templeman W (1987) Differences in sexual maturity and related characteristics between populations of thorny skate (*Raja radiata*) in the Northwest Atlantic. J Northwest Atl Fish Sci 7:155–167

Vähä JP, Primmer CR (2006) Efficiency of model-based Bayesian methods for detecting hybrid individuals under different hybridization scenarios and with different numbers of loci. Mol Ecol 15:63–72

Vähä JP, Erkinaro J, Niemelä E, Primmer CR (2007) Life-history and habitat features influence the within-river genetic structure of Atlantic salmon. Mol Ecol 16: 2638–2654

Van Oosterhout C, Hutchinson WF, Wills DPM, Shipley P (2004) MICRO-CHECKER: software for identifying and correcting genotyping errors in microsatellite data. Mol Ecol Notes 4:535–538

Vignaud TM, Maynard JA, Leblois R, Meekan MG and others (2014) Genetic structure of populations of whale sharks among ocean basins and evidence for their historic rise and recent decline. Mol Ecol 23:2590–2601

Walker PA, Heessen HJL (1996) Long-term changes in ray populations in the North Sea. ICES J Mar Sci 53: 1085–1093

Walker P, Howlett G, Millner R (1997) Distribution, movement and stock structure of three ray species in the North Sea and eastern English Channel. ICES J Mar Sci 54: 797–808

Ward RD, Woodwark M, Skibinski DOF (1994) A comparison of genetic diversity levels in marine, freshwater, and anadromous fishes. J Fish Biol 44:213–232

Warnock WG, Rasmussen JB, Taylor EB (2010) Genetic clustering methods reveal bull trout (*Salvelinus confluentus*) fine-scale population structure as a spatially nested hierarchy. Conserv Genet 11:1421–1433

Weir BS, Cockerham CC (1984) Estimating F-statistics for the analysis of population structure. Evolution 38: 1358–1370

Wienerroither R, Johannesen E, Dolgov A, Byrkjedal I and others (2011a) Atlas of the Barents Sea fishes. IMR/PINRO Joint Report Series 1-2011

Wienerroither RM, Nedreaas KH, Uiblein F, Christiansen JS, Byrkjedal I, Karamushko O (2011b) The marine fishes of Jan Mayen Island, NE Atlantic — past and present. Mar Biodiv 41:395–411

Editorial responsibility: Philippe Borsa, Montpellier, France

Submitted: September 11, 2015; Accepted: October 30, 2016
Proofs received from author(s): December 15, 2016